

Green Chemistry

Accepted Manuscript



This is an *Accepted Manuscript*, which has been through the Royal Society of Chemistry peer review process and has been accepted for publication.

Accepted Manuscripts are published online shortly after acceptance, before technical editing, formatting and proof reading. Using this free service, authors can make their results available to the community, in citable form, before we publish the edited article. We will replace this *Accepted Manuscript* with the edited and formatted *Advance Article* as soon as it is available.

You can find more information about *Accepted Manuscripts* in the [Information for Authors](#).

Please note that technical editing may introduce minor changes to the text and/or graphics, which may alter content. The journal's standard [Terms & Conditions](#) and the [Ethical guidelines](#) still apply. In no event shall the Royal Society of Chemistry be held responsible for any errors or omissions in this *Accepted Manuscript* or any consequences arising from the use of any information it contains.



www.rsc.org/greenchem

Magnetic gold (nanocat-Fe-Au) nanocatalyst: catalytic applications for the oxidative esterification and hydrogen transfer reactions

Manoj B. Gawande,^{*†a} Anuj K. Rathi,^{†a} Jiri Tucek,^a Klara Safarova,^a Nenad Bundaleski,^b Orlando M. N. D. Teodoro,^b Libor Kvitek,^a Rajender S. Varma,^{*c} and Radek Zboril^{*a}

^aRegional Centre of Advanced Technologies and Materials, Faculty of Science, Department of Physical Chemistry, Palacky University, Šlechtitelů 11, 783 71, Olomouc, Czech Republic.

^bCentre for Physics and Technological Research (CeFITec), Department of Physics, Faculdade de Ciências e Tecnologia, Universidade Nova de Lisboa, 2829-516 Caparica, Portugal.

^cSustainable Technology Division, National Risk Management Research Laboratory, US Environmental Protection Agency, MS 443, 26 West Martin Luther King Drive, Cincinnati, Ohio, 45268, USA.

[†]Both authors contributed equally

ABSTRACT

An efficient and sustainable protocol is described for the oxidative esterification of aldehydes and the reduction of aromatic nitro compounds that uses magnetically separable and reusable maghemite-supported gold nanocatalyst (nanocat-Fe-Au) under mild conditions. The complex chemical, morphological, structural and size analyses, including e.g. XPS, HRTEM, in-field Mössbauer spectroscopy and HRTEM, revealed that the hybrid material is composed of well-defined stoichiometric maghemite support (20-30 nm) decorated with ultrasmall (5-6 nm) gold nanoparticles. The hybrid catalytic system containing 4 wt% of nanogold has been generated using simple impregnation methods in aqueous medium from readily available starting materials and was recycled five times without any significant loss in catalytic activity; high yields, 40-95% and 83-94% for oxidative esterification and reduction reactions, respectively, were obtained.

Key words: *Maghemite-Au nanoparticles, Recyclable catalysts, Oxidative esterification, Reduction reaction, Sustainable protocol.*

Introduction

Sustainable organic transformations have a unique opportunity to make significant contributions in various arenas especially in pharmaceuticals and fine chemical industries and academics as well. Sustainable transformations have become one of the utmost scientific challenges due to the environmental, health and societal concerns. Consequently, it is imperative need to develop simple, efficient, and benign synthetic procedures that minimize the use of organic solvents and toxic reagents.¹ It is well-known that organic transformations without catalysts, solvent or conducted under aqueous medium are the prime choice of researchers.² This benign approach (no catalyst and solvent), however, does not work for all type of reactions, and often requires catalysts for desirable outcome of reactions in an efficient fashion. It is prudent, therefore, to design an inexpensive, greener and most importantly, a reusable and recyclable nanocatalyst;³ green and sustainable approach is an ideal forum that is pollution preventive and protects the environment by reducing or eliminating the use of hazardous substances, generation of unwanted materials, volatile organic compounds, and by-product formation.⁴

Solid-supported nanocatalysts have garnered great interest lately owing to their unique characteristics and remarkable potential in a variety of important organic transformations and sustainable technologies.^{5,6} Immobilization of metals on the surface of inert supports has recently been of interest to chemists, because these supported metal/metal oxide-supported catalysts have performed well, when compared to component metals or metal oxides.^{3b,3c,7} During the last decade, nanocatalysis by metal/metal oxide-supported catalysts has been on the forefront especially with noble metal (Pd, Pt and Au) supported catalysts which are becoming an integral part of selective organic methodologies and catalytic reactions. Gold metal/nanoparticles and supported-gold nanoparticles have acquired a special place among noble metals, due to their reactivity and they are being successfully employed in a variety of catalytic applications;⁸ metal oxide supported Au NPs (Au/MgO or TiO₂ or iron oxide etc.) with controllable shape can be prepared by the adsorption or deposition-precipitation methods, among others.^{3b, 8b,9}

Earth-abundant, iron oxide (e.g. such as magnetite, maghemite and hematite) have been well investigated as a catalysts or supports for various important organic syntheses.^{4,10} They are often adorned with metals, organoligands and metal *N*-heterocyclic carbenes as magnetically reusable nanocatalysts thus promoting the use of nanocatalysts for sustainable organic reactions.

Maghemite ($\gamma\text{-Fe}_2\text{O}_3$) has been explored due to its abundance and benign properties¹¹ and its proven biocompatibility has a promising potential to revolutionize various applications ranging from biomedicine and biosensor to in-situ remediation material¹² circumventing toxicity issues caused by previously reported support materials. Another advantage of maghemite as a support material stems from being superparamagnetic if the particle size falls below a threshold value; this can provide more convenient, efficient, and less expensive way for the collection of magnetic particles, especially in high gradient magnetic separation and nanocatalysis to support the homogeneous metals and organic ligands on the surface.¹³ Efficient binding of catalysts via magnetic field can prevent loss of deposited noble metals/metals catalyst system, ultimately lowering the production cost of metal related catalyst.

In continuation of our efforts to develop greener protocols and nanocatalysis,^{14,15} herein, we disclose an efficient protocol for the oxidative esterification of aldehydes and hydrogenation of aromatic nitro compounds under benign conditions using nanocat-Fe-Au MNPs (magnetic nanoparticles); control experiments with bare iron oxide (without Au) produced no/low yields of the products. The main objective of this study was to develop a gold nanoparticle supported on earth-abundant maghemite for catalytic nitro reduction and oxidative esterification reactions.

Experimental section

Synthesis of maghemite ($\gamma\text{-Fe}_2\text{O}_3$) nanoparticles

Magnetically separable nanocat-Fe-Au was prepared by the chemical co-precipitation method. Typically, $\text{FeSO}_4 \cdot 7\text{H}_2\text{O}$ (6.06 g, 21.79 mmol) and $\text{FeCl}_3 \cdot 6\text{H}_2\text{O}$ (11.75 g, 45.08 mmol) were dissolved in 100 mL of deionised water (previously degassed with nitrogen) under N_2 atmosphere. The resulting mixture was stirred for 15 min and heated at 60 °C under vigorous stirring. When temperature reached to 60 °C, aqueous NH_4OH (25 mL, 25-28% w/w) was added drop wise, a black precipitate was immediately formed and heating continued for 2h under N_2 atmosphere. After vigorous stirring for 2 h, the precipitate was magnetically separated and washed thoroughly with water until the supernatant liquor reached neutrality. The obtained material was dried in oven at 100 °C for 12 h and 75% yield of maghemite was observed.

Preparation of nanocat-Fe-Au catalyst

The synthesized magnetically separable maghemite (3g) and gold(III) chloride trihydrate ($\text{HAuCl}_4 \cdot 3\text{H}_2\text{O}$, to get 5 wt% of Au on maghemite) were stirred at room temperature in aqueous solution (80 mL) for 1 h. After impregnation, the suspension was adjusted to pH 12-13 by adding sodium hydroxide (1.0 M) and further stirred for 20 h. The aqueous layer was decanted with the help of external magnet and obtained

material was washed with distilled water (5 x 50 mL) and dried under vacuum at 60 °C for 12 h to afford solid material. The Au content was found to be 3.94% as determined by ICP-AES and the yield nanocat-Fe-Au was found to be 98%.

General procedure for oxidative esterification reaction

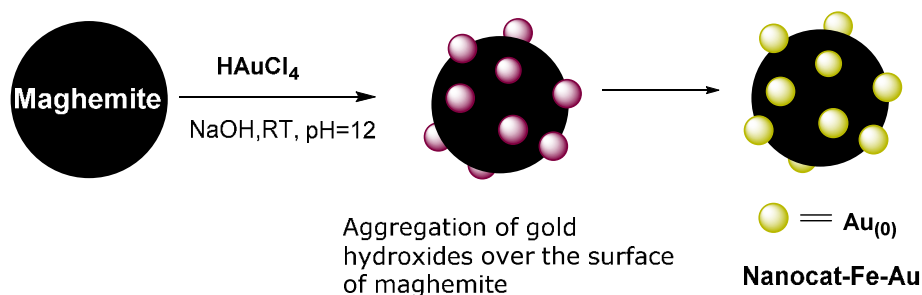
To a stirred mixture of aldehyde (1 mmol) in methanol (3 mL), potassium carbonate (10 mol%) was added followed by nanocat-Fe-Au catalyst (50 mg). The resulting mixture was stirred at 80 °C under O₂ and progress of the reaction was monitored by TLC (silica gel; hexane/ethyl acetate). After completion of the reaction, the volatiles were removed under reduced pressure and obtained material was diluted with water and extracted with ethyl acetate (3 X 20 mL). The combined ethyl acetate fractions were washed with brine, dried, and concentrated under reduced pressure by using a rotatory evaporator. The crude product was purified by column chromatography (silica 230–400; n-hexane/ethyl acetate mixture) to afford the desired product.

General procedure for hydrogenation reaction

To a stirred mixture of nitro compound (1 mmol) in ethanol (2 mL), ammonium formate (8 mmol) was added followed by the addition of catalyst (80 mg). The resulting mixture was stirred at 70 °C for appropriate time (Table 4). The progress of the reaction was monitored by TLC (silica gel; hexane/ethyl acetate). The solvent was removed under reduced pressure and obtained material was diluted with water and extracted with ethyl acetate (3X 20 mL). The combined organic layer was washed with brine, dried, and the solvent removed under reduced pressure by using a rotatory evaporator. The crude product was purified by column chromatography (silica 230–400; n-hexane/ethyl acetate mixture) to afford the amine product.

Results and discussion

Nanocat-Fe-Au catalyst was prepared by the wet impregnation method followed by chemical reduction (Scheme 1) and was completely characterized by X-ray diffraction (XRD), X-ray photoelectron spectroscopy (XPS), inductive coupled plasma-atomic emission spectroscopy (ICP-AES), transmission electron microscopy (TEM), field-emission gun, scanning electron microscopy, electron dispersive spectrometry (FEG-SEM-EDS), Mössbauer spectroscopy and high angle annular dark-field scanning transmission electron microscopy (HAADF-STEM).



Scheme 1. Synthesis of nanocat-Fe-Au MNPs

All the XRD peaks at $2\theta = 220^\circ$, 311° , 400° , 422° , 511° , and 440° could be identified with maghemite ($\gamma\text{-Fe}_2\text{O}_3$) structure (Figure 1). Although Fe_3O_4 and $\gamma\text{-Fe}_2\text{O}_3$ have the same spinel arrangement and their XRD peak positions are quite close to each other, further characterization (XPS and Mössbauer), showed clearly that the sample does not contain Fe_3O_4 and correspond to maghemite.

The prominent XRD peaks of Au on nanocat-Fe-Au were clearly observed at $2\theta = 111^\circ$, 200° , 220° , 311° , and 222° ; the crystallite size of the magnetite and gold determined by Debye Scherrer equation was found to be 17.2 nm and 4.0 nm respectively. From XRD analysis, the % of gold found be 4%, which is relatively agreement with ICP-AES (3.94%).

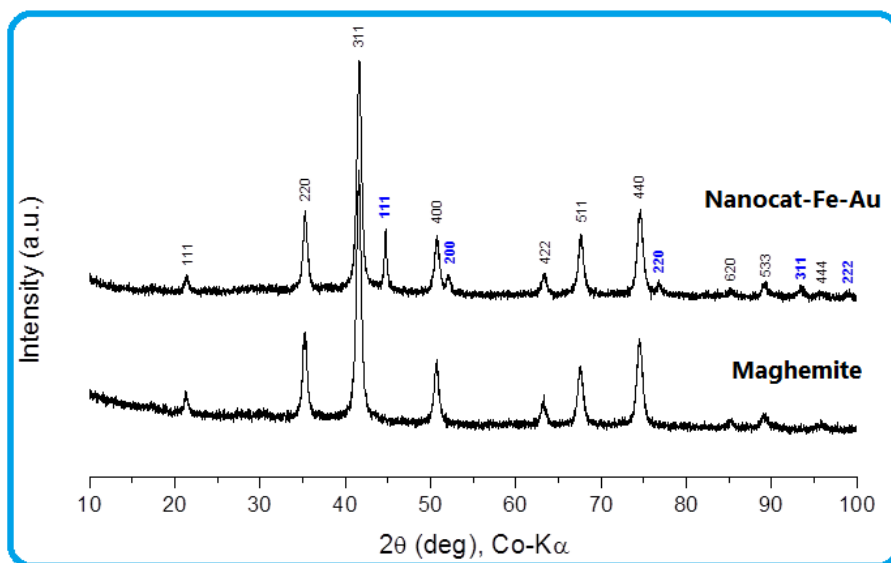


Figure 1. XRD patterns of maghemite ($\gamma\text{-Fe}_2\text{O}_3$) support (down) and nanocat-Fe-Au (up). Blue diffraction lines correspond to gold.

The XPS spectrum of Au 4f line is shown in Figure 2, after correcting the energy axis to compensate the charging problems. The position of Au 4f_{7/2} line is at 83.9 eV, perfectly matching to that of the metallic gold at 83.96 eV.¹⁸

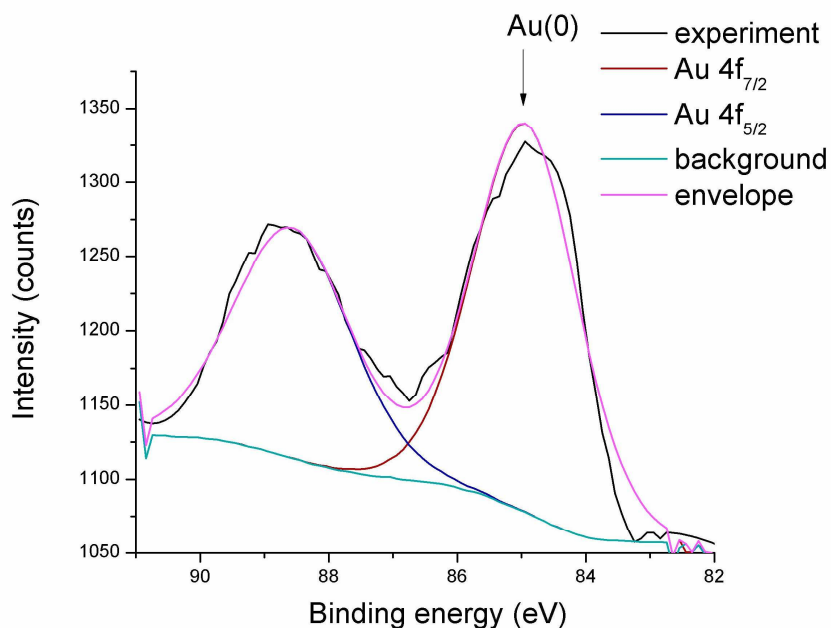


Figure 2. XPS spectrum of Au 4f line taken from nanocat-Fe-Au. The position of the Au 4f_{7/2} line for the metallic gold is denoted by arrow.

From XPS spectrum it clearly indicates that the position of the peak 1 is at 709.7 eV having excellent agreement with the peak 1 position for Fe₂O₃ at 709.8 eV. Additionally, almost perfect match between the shapes of the fitted and experimental Fe 2p_{3/2} line is obtained. All this clearly suggests that iron at the surface of nanocat-Fe-Au is present as Fe₂O₃ (See SI, Figure 2).^{18,19}

In order to get a deeper insight into the chemical nature and magnetic properties of iron oxide phase, ⁵⁷Fe Mössbauer spectroscopy was deployed. The measured Mössbauer spectra of the nanocat-Fe-Au sample are shown in Figure 3 and values of the Mössbauer hyperfine parameters, derived from spectra fitting, are listed (See SI, Table 1).

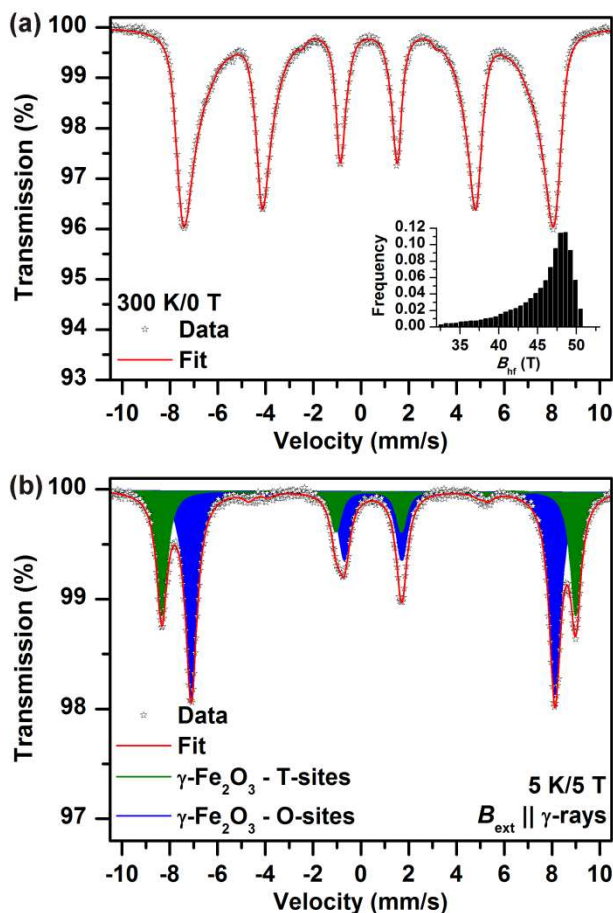


Figure 3. ^{57}Fe Mössbauer spectra of the nanocat-Fe-Au sample, recorded (a) at room temperature and without an external magnetic field and (b) at a temperature of 5 K and in an external magnetic field of 5 T.

At room temperature, the ^{57}Fe Mössbauer spectrum of the nanocat-Fe-Au sample shows only one sextet (see Figure 3a) with the values of the Mössbauer hyperfine parameters (see SI, Table 1) resembling those reported for $\gamma\text{-Fe}_2\text{O}_3$. Due to the non-Lorentzian profile of the Mössbauer resonant lines, a distribution of the hyperfine magnetic field (B_{hf}) was used when correctly fitting the spectrum. This feature is often observed for a system made up of ultrafine magnetic nanoparticles exhibiting collective magnetic excitations.²⁰ This phenomenon emerges as the nanoparticle system approaches the blocking temperature (T_{B}), i.e., a transition from the low-temperature magnetically blocked state to the superparamagnetic regime, when superspins of nanoparticles rotate around the particle easy axis of magnetization, resulting in a decrease in B_{hf} . Thus, from the viewpoint of the Mössbauer technique (with a characteristic measuring time of $\sim 10^{-8}$ s), T_{B} of the nanoparticle assembly studied is above the room temperature, implying indirectly that the average size of nanoparticles is higher than ~ 15 nm. On lowering the temperature (5 K)

and applying an external magnetic field (5 T), the Mössbauer resonant lines further split up and two sextet components appear (see Figure 3b). One sextet component with lower isomer shift (δ) and higher effective hyperfine magnetic field (B_{eff}) value can be ascribed to the tetrahedral (T) sites of the γ -Fe₂O₃ spinel crystal structure whereas the other sextet with higher δ and lower B_{eff} value belongs to the γ -Fe₂O₃ octahedral (O) sites (see SI, Table 1).²¹ Note that the spectral T:O ratio is very close to 3:5 (see Table 1) as expected for ideally stoichiometric γ -Fe₂O₃ in which Fe³⁺ ions occupy all T sites and 5/3 of O sites with 1/3 of O sites leaving vacant.²¹ The isomer shift values of both sextets fall in the range reported for a high-spin ($S = 5/2$) Fe³⁺ valence state;²² as no other spectral components are observed, the sample is of single-phased character without any admixtures of iron oxide origin.

Figure 4 shows TEM image, EDS profile and high angle annular dark-field scanning transmission electron microscopy (HAADF-STEM) images of nanocat-Fe-Au composite nanoparticles. Transmission electron microscope (TEM) analysis of nanocat-Fe-Au nanoparticles reveals that the overall diameter of the as-synthesized nanocat-Fe-Au(0) nanoparticles is in the range 20-30 nm meaning the size of magnetic support (maghemite) (Figure 4a), and EDS profile clearly indicates the presence of Fe and Au species in the catalysts. It could be clearly seen from element mapping that the element of Au, Fe, and O truly existed in the sample. The element mapping of C is not shown because a large amount of C existed in the support film of the TEM grid. As depicted in scheme 1, gold nanoparticles are distributed on the surface of maghemite; it is evidently confirmed by HAADF-STEM images (Figure 4, c- f).

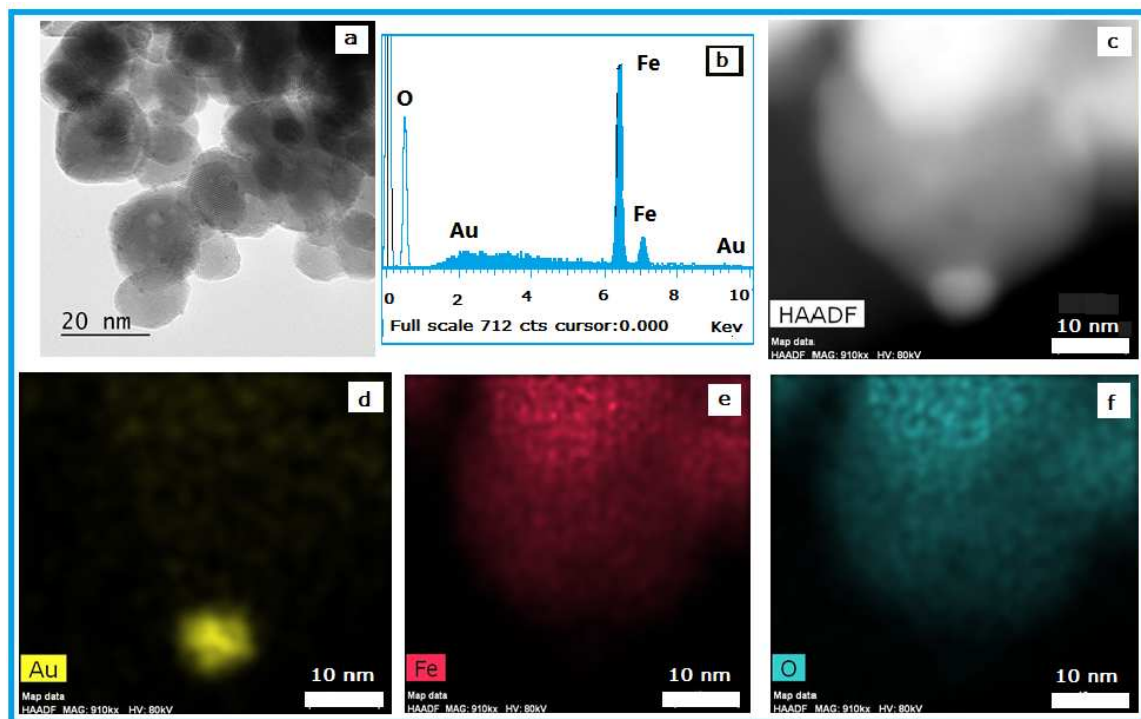
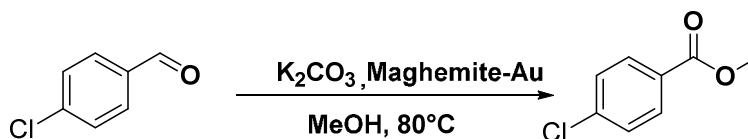


Figure 4. a) TEM images of nanocat-Fe-Au in different magnification of single nanoparticle showing gold nanoparticle. b) EDS spectrum which indicates the presence of gold; High angle annular dark-field scanning transmission electron microscopy (HAADF-STEM) of nanocat-Fe-Au; a) HAADF image of nanocat-Fe-Au at 20 nm; b) HAADF image of nanocat-Fe-Au at 10 nm ; c) HAADF image showing gold; d) HAADF image showing Fe ; e) HAADF image showing O ; f) HAADF image of showing Au, Fe and O together in one nanoparticle of nanocat-Fe-Au.

The catalytic activity of nanocat-Fe-Au was evaluated for the direct esterification of aldehydes. Initially, the reaction of 4-chloro benzaldehyde in methanol was carried out without an additive in the presence of 50 mg nanocat-Fe-Au under O_2 atmosphere at 80 °C for 7 h; no product was formed (Table 1, entry 1). With K_2CO_3 , this model reaction provided 50 % yield after 7 h (Table 1 and entry 3); even after 12 h, the corresponding product yield was not increased; but with 10 mol% K_2CO_3 , 95% yield was obtained (Table 1, entry 4). The addition of a base is important to obtain the corresponding product; reaction carried out under similar condition without base and without catalyst delivered no product. After screening for different bases such as, K_3PO_4 , KOAc, CS_2CO_3 , and K_2CO_3 , it was found that K_2CO_3 and CS_2CO_3 were effective bases for this conversion (Table 1, entries 4 and 7). With K_3PO_4 , good yield of the product was obtained and with KOAc the corresponding product 4-chloro methyl benzoate, was obtained in only 10 %. After optimizing the reaction conditions, the catalytic efficiency of nanocat-Fe-Au MNPs was further

explored with other substrates bearing electron donating and electron withdrawing groups with good to excellent yield (Table 2). It was observed that the deactivating substituents *p*-nitro- and *m*-bromo-, slows the reaction rate affording the 84% and 40% yields, respectively (Table 2, entries 4 and 6).

Table 1. Optimization of the reaction^a



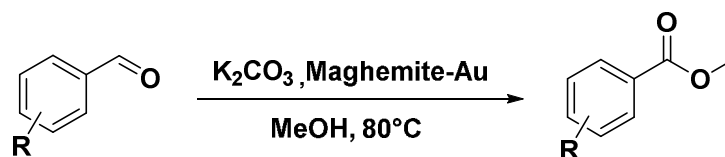
Entry	Catalyst	Time	Additive	Isolated Yield%
1	nanocat-Fe-Au	12 h	-	NR ^b
2	-	12 h	4 mol% K ₂ CO ₃	NR ^c
3	nanocat-Fe-Au	12 h	4 mol% K ₂ CO ₃	50
4	nanocat-Fe-Au	7 h	10 mol% K ₂ CO ₃	95
5	nanocat-Fe-Au	7 h	10 mol% K ₃ PO ₄	70
6	nanocat-Fe-Au	7 h	10 mol% KOAc	10
7	nanocat-Fe-Au	7 h	10 mol% Cs ₂ CO ₃	92

^a**Reaction conditions.** 4-chlorobenzaldehyde (1 mmol), K₂CO₃ (10 mol%), nanocat-Fe-Au (50 mg), MeOH (3 mL), O₂.

^bNo additive

^cNo catalyst

^dIsolated compound

Table 2. Maghemite-Au catalyzed oxidative esterification reaction of aldehydes

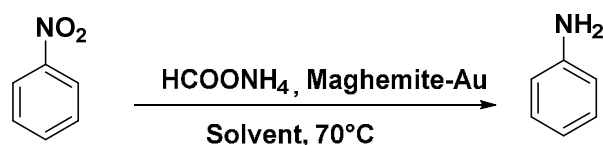
Entry	Substrates	Time (h)	Product	Isolated Yield %
1		7		94
2		7		95
3		7		95
4		10		84
5		8		83
6		12		40

Reaction condition: Aldehyde (1 mmol), K_2CO_3 (10 mol %), nanocat-Fe-Au (50 mg), MeOH (3 mL), O_2 .

Encouraged by this excellent catalytic activity of nanocat-Fe-Au for oxidative esterification of aldehydes, the catalyst was deployed for hydrogenation of nitrobenzene in benign reaction medium. The investigation was initiated with nanocat-Fe-Au and nitrobenzene as a model substrate (Table 3). It was noted that the bare iron oxides did not work for the reaction (Table 4, entry 1); the nanocat-Fe-Au without additive does not work either (Table 3, entry 2). The catalyst showed good catalytic performance in reduction reaction employing HCOONH_4 as a hydrogen source under ambient conditions (Table 4, entry

4, 5). Notably, the reduction of nitro compounds does not occur even with a large amount of HCOONH_4 without the Fe_3O_4 -Au catalyst (Table 3, entries 6, 7).

Table 3. Optimization of reaction^a



Entry	Solvent	Catalyst	Time	Yield ^d %
1	EtOH	Iron oxide	12 h	NR
2	H ₂ O	nanocat-Fe-Au	4 h	NR
3	EtOH:H ₂ O (1:1)	nanocat-Fe-Au	8 h	50
4	EtOH	nanocat-Fe-Au 100 mg	4 h	92
5	EtOH	nanocat-Fe-Au 80 mg	4 h	92
6	EtOH	-	4 h	NR ^b
7	EtOH	nanocat-Fe-Au 80 mg	4 h	NR ^c

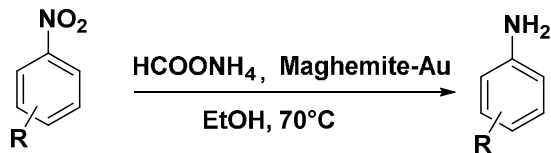
^a**Reaction conditions:** Nitro compound (1 mmol), HCOONH_4 (8 mmol), nanocat-Fe-Au (80 mg; 1.60 mol % of Au), solvent (2 mL), Temp 70°C.; NR – No reaction

^bNo catalyst was added; HCOONH_4 (15 mmol)

^cNo additive was added

^dIsolated yield

In addition, the nanocat-Fe-Au in the absence of HCOONH_4 was ineffective under the same reaction conditions, indicating that ammonium formate is necessary to drive the reduction process (Table 3, entry 7). Controlled experiments validate that the $\bullet\text{CO}_2^-$ radicals, formed by the dehydrogenation of the HCOONH_4 , are the main active species for the reduction of nitro compounds. Initially, the reaction was carried out using 100 mg catalyst, but finally optimized with 80 mg loading. It was observed that water and mixture of ethanol: water (1:1) was not compatible for this transformation. After optimization of the reaction conditions, the catalytic efficiency of nanocat-Fe-Au was further explored with other nitro substrates (Table 4). It was noted that these reduction reactions with nanocat-Fe-Au exhibit excellent activity and selectivity (80-94%) with various functional groups (Table 4, entries 2-6).

Table 4. Hydrogenation of nitro compounds

Entry	Nitro compound	Time (h)	Products	Isolated Yield (%)
1		4		94
2		3		88
3		4		83
4		4		84
5		8		88
6		8		88

Reaction condition: Nitro compound (1 mmol), HCOONH₄ (8 mmol), nanocat-Fe-Au (80 mg), EtOH (3 mL), Temp 70°C.

To validate the heterogeneous nature of the reaction, a standard leaching experiment was conducted by the hot filtration method. The model reaction of oxidative esterification of 4-chloro benzaldehyde continued for 30 minutes in the presence of the nanocat-Fe-Au at 80 °C. The hot filtered reaction mixture was then stirred without catalyst for 7 hours. Notably, no formation of the corresponding product was observed even after 12 hours, indicating that no homogeneous catalyst was involved. Inductively coupled plasma atomic emission spectra (ICP–AES) analysis of the filtrate (hot) revealed the absence of Fe and Au species in the filtrate. The stability of nanocat-Fe-Au was assessed for the oxidative esterification of 4-chloro benzaldehyde to corresponding product by magnetic recycling and reuse of the catalyst five times without any significant loss of the catalytic activity.

After completion of the reaction and between each cycle, the nanocatalyst could be easily separated by a simple decantation using an external magnet, washed with ethyl acetate, dried under vacuum, and subjected to the next cycle. Notably, after the 5th cycle negligible loss in the yield was observed (after first cycle 92 % and after 5 cycle 88 %; See SI, Table 2). To ascertain the robust nature and the versatility of nanocat-Fe-Au; after testing the recyclability for oxidative esterification reaction of benzaldehyde, the same reused catalyst was alternatively employed for reduction reaction. Further deployment again for oxidative esterification reaction and vice versa was successful; in all cases, we observed quantitative yields of the corresponding products. We have also tested sequential recyclability for the reduction of nitrobenzene; it is important to note that slight loss in the yield of aniline was observed (after first cycle 94% and after 5 cycles 89%; see SI, Table 3).

Conclusions

Recyclable nanocat-Fe-Au is shown to catalyze the oxidative esterification of aldehydes and reduction of aromatic nitro compounds. The detailed experimental investigation revealed that the reaction proceeded via heterogeneous catalysis as we could not identify the soluble species (Fe and Au) in the reaction by ICP-AES analysis. The advantages offered by this general procedure are operational simplicity, applicability to oxidative esterification and the reduction reaction, and high yields of products generated. This greener protocol enables easy recyclability of the catalyst, measured up to five times without loss of efficiency, and uses benign reaction medium. The reported results open up the possibility for the use of nanocat-Fe-Au, for other organic transformations.

Corresponding Authors

*Email- manoj.gawande@upol.cz (MBG); Varma.Rajender@epa.gov (RSV); radek.zboril@upol.cz(RZ)

Acknowledgment

The authors gratefully acknowledge the support by the Operational Program Research and Development for Innovations -European Regional Development Fund (project CZ.1.05/2.1.00/03.0058), by the Operational Program Education for competitiveness - European Social Fund (project CZ.1.07/2.3.00/30.0041) of the Ministry of Education, Youth and Sports of the Czech Republic, by the Technology Agency of the Czech Republic "Competence Centres" (project TE01010218) and by the Portuguese Research Grant Pest-OE/FIS/UI0068/2011.

References

- 1 (a) P.T. Anastas, N. Eghbali, *Chem. Soc. Rev.*, 2010, **39**, 301-312; (b) R. S. Varma, *Green Chem.*, 2014, **16**, 2027-2041; (c) C.J. Li, *Acc. Chem. Res.* 2010, **43**, 581-590.
- 2 (a) M. B. Gawande, V. D. B. Bonifacio, R. Luque, P. S. Branco, R. S. Varma, *Chem. Soc. Rev.*, 2013, **42**, 5522-5551; (b) M. B. Gawande, V. D. B. Bonifácio, R. Luque, P. S. Branco, R. S. Varma, *ChemSusChem*, 2014, **7**, 24-44.
- 3 (a) P. T. Anastas, L. B. Bartlett, M. M. Kirchhoff, T. C. Williamson, *Catal. Today*, 2000, **55**, 11-22; (b) A. Corma, H. Garcia, *Chem. Soc. Rev.*, 2008, **37**, 2096-2126; (c) S. E. Davis, M. S. Ide, R. J. Davis, *Green Chem.*, 2013, **15**, 17-45.
- 4 M. B. Gawande, P. S. Branco, R. S. Varma, *Chem. Soc. Rev.*, 2013, **42**, 3371-3393.
- 5 M. B. Gawande, A. Velhinho, I. D. Nogueira, C. A. A. Ghumman, O. Teodoro, P. S. Branco, *Rsc Adv.*, 2012, **2**, 6144-6149.
- 6 (a) R. van Heerbeek, P. C. J. Kamer, P. van Leeuwen, J. N. H. Reek, *Chem. Rev.*, 2002, **102**, 3717-3756; (b) M. B. Gawande, S. N. Shelke, P. S. Branco, A. Rathi, R. K. Pandey, *Appl. Organomet., Chem.*, 2012, **26**, 395-400.
- 7 (a) M. B. Gawande, R. K. Pandey, R. V. Jayaram, *Catal. Sci. Technol.*, 2012, **2**, 1113-1125; (b) A. Schatz, O. Reiser, W. J. Stark, *Chem. Eur. J.*, 2010, **16**, 8950-8967.
- 8 (a) J. C. Bauer, G. M. Veith, L. F. Allard, Y. Oyola, S. H. Overbury, S. Dai, *ACS Catal.*, 2012, **2**, 2537-2546; (b) T. Risse, S. Shaikhutdinov, N. Nilius, M. Sterrer, H.-J. Freund, *Acc. Chem. Res.*, 2008, **41**, 949-956.
- 9 (a) M.C. Daniel, Astruc D. (b) M. Grzelczak, J. Perez-Juste, P. Mulvaney, L. M. Liz-Marzan, *Chem. Soc. Rev.*, 2008, **37**, 1783-1791; (c) Z. Ma, S. Dai, *ACS Catal.*, 2011, **1**, 805-818.
- 10 (a) S. R. Kale, S. S. Kahandal, M. B. Gawande, R. V. Jayaram, *Rsc Adv.*, 2013, **3**, 8184-8192; (b) V. Polshettiwar, B. Baruwati, R. S. Varma, *Chem. Commun.*, 2009, 1837-1839; (c) R. B. N. Baig, R. S. Varma, *Chem. Commun.*, 2012, **48**, 2582-2584; (d) B. R. Vaddula, A. Saha, J. Leazer, R. S. Varma, *Green Chem.*, 2012, **14**, 2133-2136; (e) C. O' Dalaigh, S. A. Corr, Y. Gun'ko, S. J. Connon, *Angew. Chem., Int. Ed.*, 2007, **46**, 4329-4332; (f) M. B. Gawande, P. S. Branco, I. D. Nogueira, C. A. A. Ghumman, N. Bundaleski, A. Santos, O. Teodoro, R. Luque, *Green Chem.*, **2013**, **15**, 682-689; (g) P.-H. Li, B.-L. Li, Z.-M. An, L.-P. Mo, Z.-S. Cui, Z.-H. Zhang, *Adv. Synth. Catal.*, 2013, **355**, 2952-2959; (h) F. Rajabi, N. Karimi, M. R. Saidi, A. Primo, R. S. Varma, R. Luque, *Adv. Synth. Catal.*, 2012, **354**, 1707-1711; (i) K. V. S. Ranganath, J. Kloesges, A. H. Schafer, F. Glorius, *Angew. Chem., Int. Ed.*, 2010, **49**, 7786-7789; (j) R. Cano, D. J. Ramon, M. Yus, *J. Org. Chem.*, 2010, **75**, 3458-3460; (k) R. Hudson, A. Riviere, C. M. Cirtiu, K. L. Luska, A. Moores, *Chem.*

- Commun.*, 2012, **48**, 3360-3362; (l) M. Hermanek, R. Zboril, I. Medrik, J. Pechousek, C. Gregor, *J. Am. Chem. Soc.*, 2007, **129**, 10929-10936; (m) A. Rezaeifard, M. Jafarpour, P. Farshid, A. Naeimi, *Eur. J. Inorg. Chem.*, 2012, 5515-5524;
- 11 F. Nador, M. A. Volpe, F. Alonso, A. Feldhoff, A. Kirschning, G. Radivoy, *Appl. Catal. A.*, 2013, **455**, 39-45.
- 12 J. Chomoucka, J. Drbohlavova, D. Huska, V. Adam, R. Kizek, J. Hubalek, *Pharmacological Res.*, 2010, **62**, 144-149.
- 13 (a) S. Gyergyek, D. Makovec, A. Mertelj, M. Huskic, M. Drogenik, *Colloids and Surfaces a-Physicochemical and Engineering Aspects*, 2010, **366**, 113-119; (b) H. Mahmoudi, A. A. Jafari, *ChemCatChem*, 2013, **5**, 3743-3749; (c) L. Machala, J. Tuček, R. Zbořil, *Chem. Mater.*, 2011, **23**, 3255-3272.
- 14 (a) M. B. Gawande, A. K. Rath, I. D. Nogueira, R. S. Varma, P. S. Branco, *Green Chem.*, 2013, **15**, 1895-1899; (b) Z. Markova, K. Siskova, J. Filip, K. Safarova, R. Prucek, A. Panacek, M. Kolar, R. Zboril, *Green Chem.*, 2012, **14**, 2550-2558; (c) A. Panacek, R. Prucek, J. Hrbac, T. Nevecna, J. Steffkova, R. Zboril, L. Kvitek, *Chem. Mater.*, 2014, **26**, 1332-1339; (d) M. B. Gawande, S. N. Shelke, R. Zboril, R. S. Varma, *Acc. Chem. Res.*, 2014, **47**, 1338-1348.
- 15 (a) M. B. Gawande, A. Rath, I. D. Nogueira, R. S. Varma, P. S. Branco, *Green Chem.*, 2013, **15**, 1895-1899; (b) M. B. Gawande, A. K. Rath, P. S. Branco, I. D. Nogueira, A. Velhinho, J. J. Shrikhande, U. U. Indulkar, R. V. Jayaram, C. A. A. Ghumman, N. Bundaleski, O. M. N. D. Teodoro, *Chem. Eur. J.*, 2012, **18**, 12628 – 12632.; (c) M. B. Gawande, A. Rath, I. D. Nogueira, C. A. A. Ghumman, N. Bundaleski, O. M. N. D. Teodoro, P. S. Branco, *ChemPlusChem*, 2012, **77**, 865– 871; (d) M. B. Gawande, V. D. B. Bonifacio, R. S. Varma, I. D. Nogueira, N. Bundaleski, C. A. A. Ghumman, O. M. N. D. Teodoro, P. S. Branco, *Green Chem.*, 2013, **15**, 1226-1231.
- 16 O. Teodoro, J. Silva, A. M. C. Moutinho, *Vacuum*, 1995, **46**, 1205-1209.
- 17 Z. Klencsar, E. Kuzmann, A. Vertes, *J. Radioanal. Nucl. Chem. Art.*, 1996, **210**, 105-118.
- 18 NIST XPS database <http://srdata.nist.gov/xps/Default.aspx>.
- 19 M. C. Biesinger, B. P. Payne, A. P. Grosvenor, L. W. M. Lau, A. R. Gerson, R. S. Smart, *Appl. Sur. Sci.*, 2011, **257**, 2717-2730.
- 20 S. Morup, H. Topsoe, *Appl. Phys.*, 1976, **11**, 63-66.
- 21 J. Tucek, R. Zboril, D. Petridis, *J. Nanosci. Nanotechnol.*, 2006, **6**, 926-947.
- 22 Greenwood, N. N.; Gibb, T. C. Mössbauer Spectroscopy; Chapman and Hall Ltd.: London, UK, 1971.

Magnetic gold (nanocat-Fe-Au) nanocatalyst: catalytic applications for the oxidative esterification and hydrogen transfer reactions

Manoj B. Gawande,^{*†a} Anuj K. Rathi,^{†a} Jiri Tucek,^a Klara Safarova,^a Nenad Bundaleski,^b Orlando M. N. D. Teodoro,^b Libor Kvitek,^a Rajender S. Varma,^{*c} and Radek Zboril^{*a}

A sustainable protocol is described for the oxidative esterification of aldehydes and the reduction of aromatic nitro compounds that uses magnetically separable and reusable maghemite-supported gold nanocatalyst (nanocat-Fe-Au); hybrid catalytic system, containing 4 wt% of nanogold, generated via simple impregnation method was recycled five times without any significant loss in catalytic activity.

